Interfacial Interactions of Ceramide with Dimyristoylphosphatidylcholine: Impact of the N-Acyl Chain

Juha M. Holopainen,* Howard L. Brockman,† Rhoderick E. Brown,† and Paavo K. J. Kinnunen*
*Helsinki Biophysics and Biomembrane Group, Department of Medical Chemistry, Institute of Biomedicine, University of Helsinki, FIN-00014 Helsinki, Finland; and †The Hormel Institute, University of Minnesota, Austin, Minnesota 55912 USA

ABSTRACT The mixing behavior of dimyristoylphosphatidylcholine (DMPC) with either N-palmitoyl-sphingosine (C16:0-ceramide) or N-nervonoyl-sphingosine (C24:1-ceramide) was examined using monomolecular films. While DMPC forms highly elastic liquid-expanded monolayers, both neat C16:0-ceramide and C24:1-ceramide yield stable solid condensed monomolecular films with small areas and low interfacial elasticity. Compression isotherms of mixed C16:0-ceramide/DMPC films exhibit an apparent condensation upon increasing $X_{cer16:0}$ at all surface pressures. The average area isobars, coupled with the lack of a liquid-expanded to condensed phase transition as $X_{cer16:0}$ is increased, are indicative of immiscibility of the lipids at all surface pressures. In contrast, isobars for C24:1-ceramide/DMPC mixtures show surface pressure-dependent apparent condensation or expansion and surface pressure-area isotherms show a composition and surface pressure-dependent phase transition. This suggests miscibility, albeit non-ideal, of C24:1-ceramide and DMPC in both liquid and condensed surface phases. The above could be verified by fluorescence microscopy of the monolayers and measurements of surface potential, which revealed distinctly different domain morphologies and surface potential values for the DMPC/C16:0- and DMPC/C24:1-ceramide monolayers. Taken together, whereas C16:0-ceramide and DMPC form immiscible pseudo-compounds, C24:1-ceramide and DMPC are partially miscible in both the liquid-expanded and condensed phases, and a composition and lateral pressure-dependent two-phase region is evident between the liquid-expanded and condensed regimes. Our results provide novel understanding of the regulation of membrane properties by ceramides and raise the possibility that ceramides with different acyl groups could serve very different functions in cells, relating to their different physicochemical properties.

INTRODUCTION

Lipids represent the structurally most diverse class of biomolecules. Although the evolution of this diversity appears to be connected to the emergence of eukaryotes, its functional significance has remained enigmatic (Kinnunen, 1991). Comparison of the physicochemical properties of polar lipids with various headgroups has revealed a rich scale of different phases and complex phase behavior (Kinnunen and Laggner, 1991). The impact of the variation in the acyl chain lengths has received less attention and is likely to be due to the fact that except for the difference between saturated and unsaturated chains of phosphatidylcholines, for instance, their effects are more subtle. This is a particularly prominent feature of sphingolipids, which may comprise ~30% of the total lipids of the plasma membrane of eukaryotic cells. For example, SM extracted from egg is enriched in C16:0 acyl chains, whereas a significant fraction of bovine brain SM bears C24:1 chains. Possible specific roles for these lipids in cells have remained open. A large amount of evidence points to the coordinated regulation of both cholesterol and sphingomyelin levels in cells (e.g., Kolesnick, 1991) and several findings indicate the importance of sphingolipids in a number of biological events. Accordingly, ceramide has been recognized as a "second messenger" in cellular signaling cascades for the induction of apoptosis, growth, differentiation, and cell senescence (Hannun, 1996). A recent study indicates that the ceramide species involved in apoptosis of Jurkat cells is C16:0-ceramide (Thomas et al., 1999).

These and related recent findings of lipid-mediated events in cell signaling have led to the resurrection of interest in the forces and molecular interactions governing the physical properties and dynamic lateral microheterogeneity of biomembranes (Mouritsen and Kinnunen, 1996). Moreover, we have suggested that the *physiological* state of the cell is determined by the *physical* (phase) state of its membranes (Kinnunen et al., 1994) and have emphasized the significance of functional ordering in biomembranes (Kinnunen, 1991). In the plasma membrane ceramide is enriched in caveolae, 50–60-nm-diameter invaginations having distinct protein and lipid compositions (Parton et al., 1994). These sphingolipid-enriched membrane domains contain G-protein-coupled receptors and may play a role in signal transduction and endocytosis (Lisanti et al., 1994). It

Received for publication 12 April 2000 and in final form 27 September 2000.

Address reprint requests to Paavo K. J. Kinnunen, M.D., Department of Medical Chemistry, Institute of Biomedicine, P. O. Box 8 (Siltavuorenpenger 10 A), FIN-00014 University of Helsinki, Finland. Tel.: 358-9-191-8237; Fax: 358-9-191-8276; E-mail: Paavo.Kinnunen@Helsinki.Fi.

Abbreviations used: SM, sphingomyelin; C16:0-ceramide, N-palmitoyl-sphingosine; C24:1-ceramide, N-nervonoyl-sphingosine; C_S^{-1}, elastic modulus of area compressibility; DMPC, dimyristoylphosphatidylcholine; H_{II}, hexagonal phase; LE → LC, liquid-expanded to liquid-condensed phase transition; $\mu_\perp$, perpendicular surface dipole moment; NBD-PC, 1-palmitoyl-2-{12-[(7-*nitro*-2-1,3-benzoxadizole-4-yl)amino]dodecanoyl)-phosphocholine; π, surface pressure; PC, phosphatidylcholine; ΔV, surface potential; X_A, mole fraction of compound A.

0006-3495/01/02/765/11 $2.00

was shown that interleukin-1β binding to a sphingomyelin-rich plasma membrane domain with the characteristics of caveolae was accompanied by the hydrolysis of sphingomyelin to ceramide, and the formation of the latter lipid was concluded to be highly compartmentalized in the cell surface (Liu and Anderson, 1995).

Our previous differential scanning calorimetry (DSC) and fluorescence spectroscopy studies on natural ceramide in DMPC LUVs and C16:0-ceramide in 1-palmitoyl-2-oleoylphosphatidylcholine (POPC) LUVs provided evidence for ceramide-enriched microdomains in both the gel state and fluid bilayers (Holopainen et al., 1997, 1998). Similar results were also obtained for bovine brain ceramides in mixtures with dipalmitoylphosphatidylcholine (Veiga et al., 1999). DSC studies on the behavior of synthetic C16:0-ceramide have shown fully hydrated C16:0-ceramide to display a broad exotherm at ~50–70°C and an endothermic transition at 90.0°C (Shah et al., 1995). X-ray diffraction showed that the exothermic transition was accompanied by a decreased bilayer periodicity and an increased layer, as well as chain packing order. The endothermic transition was identified as a main transition and involved a decrease in bilayer thickness and a new diffuse reflection at 4.6 Å indicative of a melted chain phase. Using x-ray scattering and high-sensitivity DSC we could show that increasing C16:0-ceramide up to $X = 0.35$ in DMPC MLVs preserved the lamellar phase in these binary liposomes up to 60°C. Coexisting gel and fluid domains were observed upon increasing the mole fraction of ceramide (Holopainen et al., 2000a). It was recently shown that the bovine brain ceramide (having an N-acyl chain composition of 32% of C18:0- and 48% of 24:1-ceramide) exhibits complete or partial phase immiscibility in dipalmitoylphosphatidylcholine monolayers (Carrer and Maggio, 1999).

Using fluid giant unilamellar vesicles composed of phosphatidylcholine and sphingomyelin we demonstrated that the action of sphingomyelinase first resulted in the rapid formation of ceramide-enriched microdomains (Holopainen et al., 2000b). Interestingly, this was followed by either endocytosis-like shedding of vesicles into the interior of the giant liposome or outward budding, depending on the sidedness of the enzymatic reaction (Holopainen et al., 2000b). These observations are in keeping with a functional role for ceramide in the morphological changes of the plasma membrane occurring in apoptosis (Majno and Joris, 1995). Finally, it is also noteworthy that understanding of the biophysical properties of ceramide bears major physiological significance to dermatology. Accordingly, ceramide has been shown to be responsible for the high tolerance of skin to physical stress, thus perhaps emphasizing the importance of the intermolecular hydrogen bonding (Elias and Menon, 1991; Moore et al., 1997; Pascher, 1976).

The present investigation was undertaken to study the interactions and macroscopic ordering of two synthetic ceramides (viz. C16:0-ceramide and C24:1-ceramide, which has a *cis* double bond between carbon atoms 15 and 16) in mixed monolayers with DMPC at the air/water interface. Our results show that both mixtures show composition-dependent phase separation, while their phase behaviors differ significantly.

MATERIALS AND METHODS

Lipids

DMPC was from Sigma (St. Louis, MO) and C16:0-ceramide and C24:1-ceramide were from either Sigma or Northern Lipids Inc. (Vancouver, British Columbia, Canada). NBD-PC was obtained from Molecular Probes (Eugene, OR). Their purity was checked by thin-layer chromatography on silicic acid-coated plates (Merck, Darmstadt, Germany) using chloroform/methanol/water (65:25:4, v/v/v) for DMPC and NBD-PC, and 1,2-dichloroethane/methanol/water (90:20:0.5, v/v/v) as the solvent system for the ceramides. Examination of the plates after iodine staining revealed no impurities. Concentrations of the lipids were determined gravimetrically using a high-precision electrobalance (Cahn, Cerritos, CA).

Monolayer studies

A computer-controlled Langmuir-type film balance, calibrated with lipid standards according to their equilibrium spreading pressures (Smaby and Brockman, 1990) and housed in a laboratory equipped with a charcoal- and HEPA-filtered air supply, was used to simultaneously measure π-A and ΔV-A isotherms. All glassware used was acid-cleaned and rinsed thoroughly with chloroform/methanol (1:1, v/v). The solution of each lipid was spread in 51.7 μl aliquots onto a trough filled with ~800 ml of 10 mM phosphate-saline buffer, 1 M NaCl, pH 6.6 at 24°C. After a period of 4 min, to ensure complete evaporation of solvents, the monolayer films were compressed at a rate of <4 Å^2/molecule/min, so as to allow for the reorientation of the lipids during compression. All experiments were repeated at least once to ensure reproducibility. If subsequent isotherms differed more than 1 mN/m and/or 2 Å^2/molecule or ΔV-A behavior differed >20 mV, a third sample was analyzed.

Analysis of isotherms

Phase transitions were identified using derivatives of surface pressure with respect to area (Brockman et al., 1980) as implemented in FilmFit software (Kibron Inc., Helsinki, Finland). The value for monolayer isothermal compressibilities (C_S) for the indicated film compositions at the given surface pressures (π) were obtained from π-A data using

$$C_S = (-1/A_\pi) * (dA/d\pi)_\pi$$

where A_π is the area per molecule at the indicated surface pressure and π is the corresponding surface pressure. In order to facilitate comparison with measurements made with bilayers, we further analyzed our data in terms of the reciprocal of isothermal compressibility (i.e., C_S^{-1}), as discussed previously (Smaby et al., 1996). The higher the C_S^{-1} value the lower the interfacial elasticity. A 5-point sliding window was used to calculate the C_S^{-1} value before advancing the window one point. Each π - C_S^{-1} curve consisted of 999 C_S^{-1} values obtained at equally spaced molecular areas covering the studied surface pressure range. The data were further smoothed by the Savitzky-Golay function, which performs a local polynomial regression of 13 values around each measured data point.

Surface potential-area behavior

The ΔV-A behavior of lipid films was recorded during compression isotherms using an ionizing electrode, essentially as described previously (Brockman, 1994; Smaby and Brockman, 1992). For ideally miscible or phase-separated multicomponent monolayers, the dipole potential at any surface pressure can be calculated to be the area-weighted average of individual surface potentials of the coexisting phases at the same surface pressure,

$$\Delta V_\pi = \Delta V_0 + 37.70\mu_\perp/A_\pi \quad (1)$$

where ΔV_0 is the area-apportioned sum of the individual lipid concentration-independent components of the dipole potential and $\mu_\perp$ is the mole fraction-apportioned sum of the component dipole moments perpendicular to the plane of the interface (Smaby and Brockman, 1990, 1992).

Fluorescence microscopy of monolayers

Lateral organization of the mixed monolayers of DMPC and either C16:0- or C24:1-ceramide was observed by fluorescence microscopy and using a computer-controlled Wilhelmy-type film balance (μTrough S, Kibron Inc., Helsinki, Finland). Total surface area of the trough is 120 cm^2, and the volume of the subphase is 22 ml. The trough was mounted on the stage of an inverted microscope (Zeiss IM-35, Jena, Germany) and the quartz-glass window in the bottom of the trough was positioned over an extra long working distance 20× objective (Nikon). A 450–490 nm bandpass filter was used for excitation and a 520 nm longpass filter for emission. Images were viewed with a Peltier-cooled 12-bit digital camera (C4742–95, Hamamatsu, Japan) interfaced to a computer (Pentium 166 MHz) and running image processing software provided by the camera manufacturer (HiPic, 4.2.0). NBD-PC ($X = 0.01$) was used as a fluorescent probe. Stock solutions of the probe and the lipids, DMPC/C16:0-ceramide/NBD-PC at the indicated molar ratios (99:0:1, 49:50:1, and 9:90:1) and DMPC/C24:1-ceramide/NBD-PC (79:20:1 and 29:70:1) were prepared in chloroform and stored at −20°C. These mixtures were applied on the air-buffer (10 mM phosphate-saline buffer, 1 M NaCl, pH 6.6) interface using a Hamilton microsyringe to initial areas of 100 ± 10 Å^2/acyl chain. After an equilibration period of 10 min the monolayers were compressed symmetrically using two barriers at a rate of 2.5 Å^2/acyl chain/min. After reaching the indicated values for surface pressure (π) the compression was stopped and the monolayer was allowed to settle for 2 min before recording the image. All measurements were done at ambient temperature of 24 ± 1°C and were repeated at least twice.

RESULTS

Compression isotherms for DMPC/C16:0-ceramide and DMPC/C24:1-ceramide monolayers

In our first set of experiments we used the synthetic N-palmitoyl-sphingosine, C16:0-ceramide, and the saturated DMPC, with comparable lengths of their hydrophobic moieties. At 24°C and at all surface pressures below film collapse, neat DMPC monolayers were chain-disordered, i.e., liquid-expanded. Representative compression isotherms for mixed DMPC/C16:0-ceramide monolayers as well as neat lipids are shown in Fig. 1 *A*. The isotherms show several interesting features. First, the addition of increasing amounts of the highly condensed C16:0-ceramide does not result in the appearance of a clearly discernible liquid-expanded to liquid-condensed phase transition (LE → LC), even though the measurement temperature (≈24°C) is close to the phase transition temperature of DMPC bilayers, and increasing $X_{cer16:0}$ results in a more condensed film behavior. Phillips and Chapman (1968) showed that the monolayer liquid-expanded → liquid-condensed phase transition appears at surface pressures below monolayer collapse as the temperature is lowered below the gel- to liquid-crystalline phase transition temperature of the lipid in bilayers. It could thus be anticipated that the addition of C16:0-ceramide with its much higher transition temperature (Shah et al., 1995) would result in mixed monolayers of C16:0-ceramide and DMPC having a measurable phase transition at a surface pressure that decreases with increasing content of C16:0-ceramide. The absence of such a transition at 24°C suggests that C16:0-ceramide has little or no miscibility in DMPC monolayers. The second interesting feature of the isotherms is that above $X_{cer16:0} = 0.7$ to 0.8, the isotherms are nearly identical (Fig. 1 *A*). The absence of composition-dependence of the average molecular area suggests that in this range a single, condensed monolayer phase is present.

In theory, the collapse pressures of isotherms like those shown in Fig. 1 can indicate over what range the components are miscible (Crisp, 1949). However, in general for lipids with high collapse pressures and in particular for condensed monolayers, deducing phase behavior from compression isotherms can be misleading. To further investigate the mixing of the monolayer components, isobars of average molecular area versus monolayer composition (A vs. $X_{cer16:0}$) at surface pressures of 5, 15, 30, and 40 mN/m were constructed (Fig. 2, *left*). Comparison of the data to the predicted additive behavior is consistent with the qualitative interpretation of the π versus A isotherms given above. Particularly evident at low surface pressure, the components appear to mix up to $\sim X_{cer16:0} = 0.1$. Between $X_{cer16:0}$ of 0.1 and 0.7 (solid line connecting the data points in Fig. 2, *left*) the average area decreases linearly and then becomes constant at higher mole fractions of C16:0-ceramide. This behavior is consistent with the liquid-expanded phase of DMPC solubilizing C16:0-ceramide up to $X_{Xcer16:0} = 0.10$ and the condensed C16:0-ceramide phase solubilizing DMPC up to $X_{DMPC} = 0.30$, in keeping with DSC and x-ray data (Holopainen et al., 1997, 2000a). The composition-independence of the break points indicates that mixtures of these compositions behave as pseudo-compounds or complexes as previously observed for cholesterol-phospholipid mixtures (Radhakrishnan and McConnell, 1999). In the intermediate region of linear average molecular area-composition behavior (Fig. 2 *left*, *solid line*) the monolayer should thus consist of two immiscible pseudo-compound phases, which are liquid DMPC/C16:0-ceramide (~79:1 molar ratio) and solid DMPC/C16:0-ceramide (~73:7 molar ratio). It is of interest that after compression, ceramide containing (≥0.8) monolayers appear to remain in a condensed state even after decompression of the membrane (data not shown).

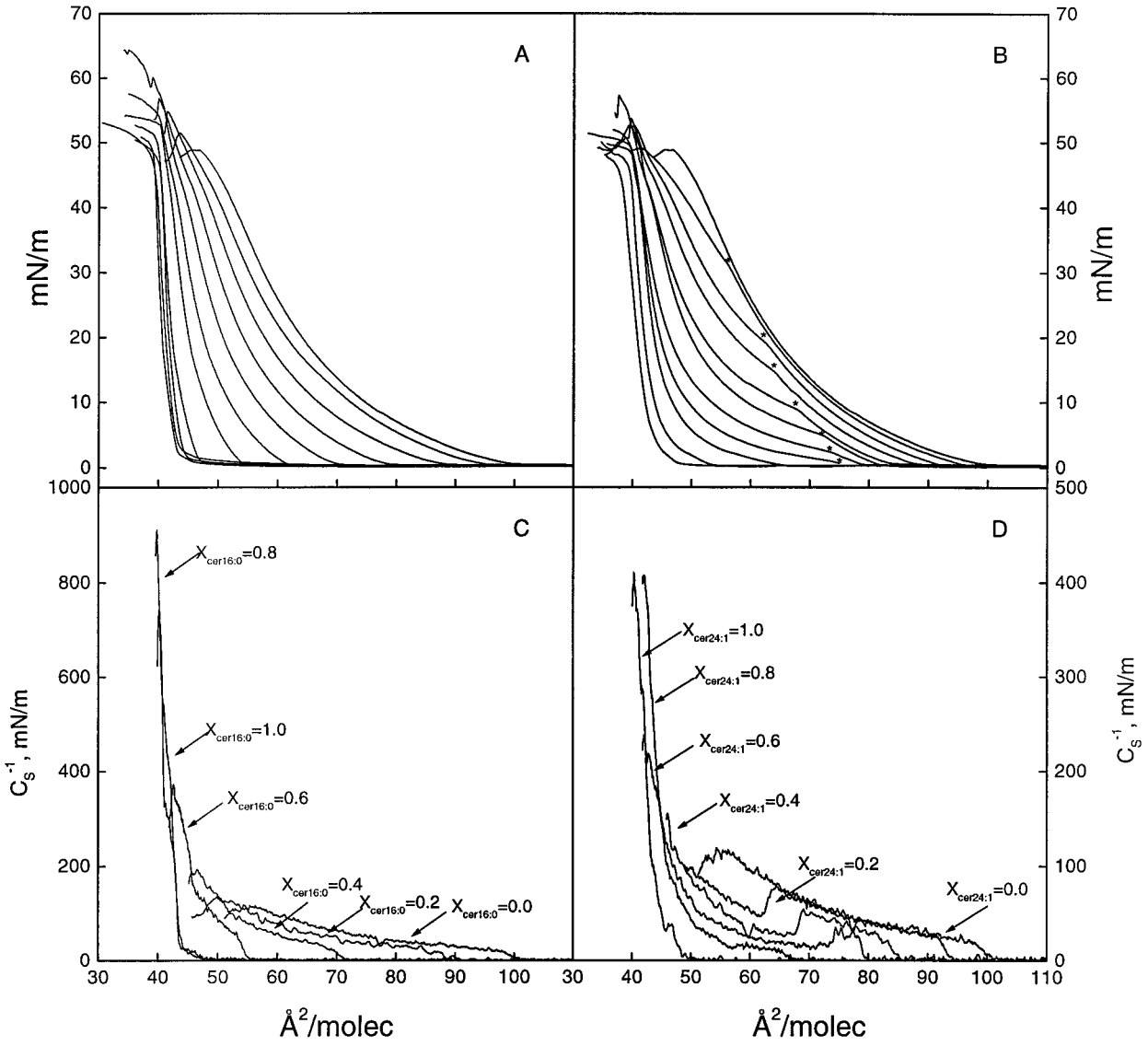

FIGURE 1 (*A*) Representative compression isotherms for DMPC with increasing concentrations of C16:0-ceramide. The mole fractions of C16:0-ceramide are from left to right 0.8, 1.0, 0.9, 0.7, 0.6, 0.5, 0.4, 0.3, 0.2, 0.1, and 0. The solution of each lipid was spread onto a trough filled with (800 ml) 10 mM phosphate-saline buffer, 1 M NaCl, pH 6.6 at 24°C. After a period of 4 min the monolayer films were compressed at a rate of <4 Å^2/molecule/min. (*B*) Compression isotherms measured for pure C24:1-ceramide and its mixtures with DMPC. The mole fractions of C24:1-ceramide are from left to right 1.0, 0.9, 0.8, 0.7, 0.6, 0.5, 0.4, 0.3, 0.2, 0.1, and 0. The conditions were as for Fig. 1. The asterisks indicate the position of the observed phase transitions. (*C*) The C_S^{-1} versus mean molecular area for $X_{cer16:0} = 0$, 0.2, 0.4, 0.6, 0.8, and 1.0, calculated from the graphs in *A*. (*D*) The data in *B* were used to calculate the C_S^{-1} versus mean molecular area for $X_{cer24:1} = 0$, 0.2, 0.4, 0.6, 0.8, and 1.0. All experiments were repeated at least once to ensure reproducibility. If subsequent isotherms differed by >1 mN/m and/or 2 Å^2/molecule, a third sample was analyzed.

We then proceeded to study the synthetic C24:1-ceramide, with an 18-carbon sphingosine base and C24:1 chain as the N-acyl chain. Monolayers of this lipid are liquid-condensed or solid-condensed with a small headgroup area, ~38 Å^2/molecule. Representative compression isotherms of DMPC/C24:1-ceramide mixtures are compiled in Fig. 1 *B*. In contrast to the DMPC/C16:0-ceramide films a clear phase transition is evident already at $X_{cer24:1} = 0.1$, and increasing $X_{cer24:1}$ causes this transition to shift to lower surface pressures (marked with asterisks in Fig. 1 *B* and also included into Fig. 2, *right*). At $X_{cer24:1} \geq 0.8$ the above discontinuity can no longer be resolved. To quantitatively compare the apparent condensing and expanding effects of C24:1-ceramide in a DMPC monolayer we determined the additivity of mean molecular areas at four different surface pressures, viz. 5, 15, 30, and 40 mN/m (Fig. 2, *right*). In contrast to C16:0-ceramide, substantial *positive* deviations at 5 mN/m for area additivity were evident at $X_{cer24:1} < 0.6$. Up to $\pi = 15$ mN/m a positive deviation is still observed when $X_{cer24:1} < 0.4$, while increasing $X_{cer24:1}$ further results

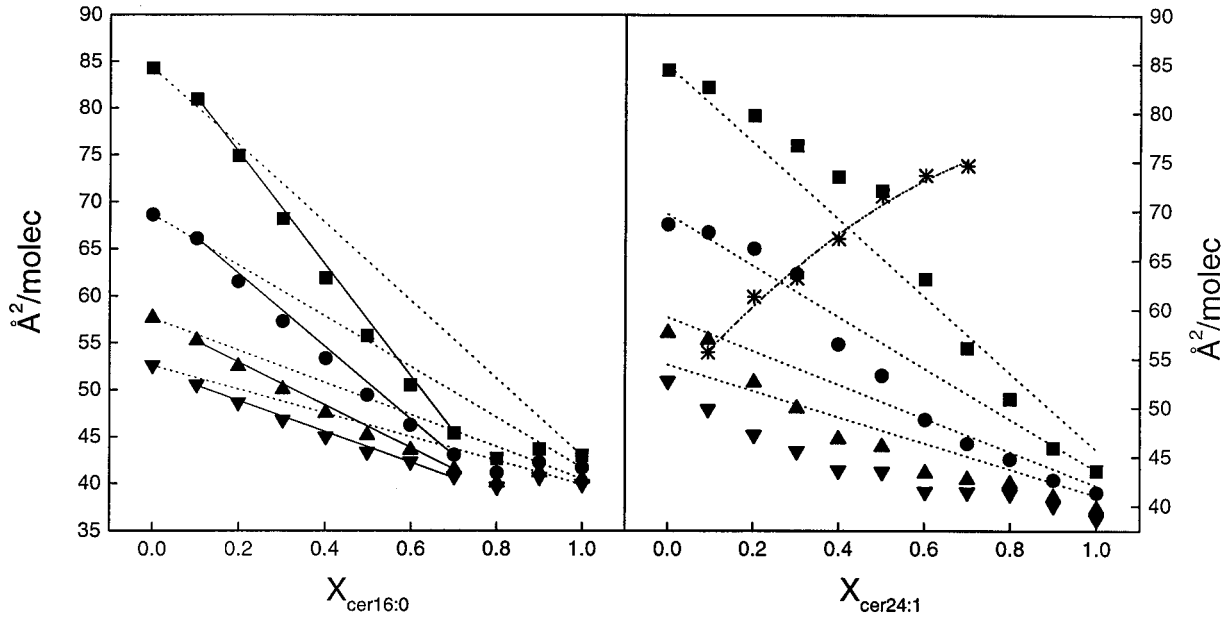

FIGURE 2 Mean molecular areas for binary mixtures of C16:0-ceramide and DMPC (*left*) and C24:1-ceramide/DMPC binary alloys (*right*) at 5 (■), 15 (●), 30 (▲), and 40 (▼) mN/m. The asterisks (*right*) indicate the position of the phase transition observed from Fig. 1 *B*. The data were taken from the graphs illustrated in Figs. 1 *A* and 2 *left*.

in a negative deviation from the ideal area additivity. Further increase in surface pressure ($\pi > 30$ mN/m) results in negative deviation from ideal additivity of surface areas. The latter indicates miscibility of the components in the condensed state. To conclude, the above behavior suggest that the two components are partially miscible in both the liquid-expanded and condensed phases, whereas a composition and lateral pressure-dependent two-phase region is evident between the liquid-expanded and condensed regimes. Notably, C24:1-ceramide and DMPC do not form pseudo-complexes similar to those observed for the mixed films of DMPC and C16:0-ceramide.

Interfacial elastic moduli of area compressibility of DMPC/ceramide films

The C_S^{-1} versus A behavior was determined from the π-A data as described under Materials and Methods (Fig. 1 *C*). C_S^{-1} for pure DMPC (108 mN/m) at 30 mN/m reflects the fluid nature of the lipid packing state (Smaby et al., 1997). Interestingly, upon increasing $X_{cer16:0}$ up to 0.4 the average molecular area decreases, while the in-plane elasticity remains relatively unaffected (Fig. 3). Thereafter, a further increase in $X_{cer16:0}$ results in a dramatic enhancement in C_S^{-1}. The value of $X_{cer16:0}$ at which C_S^{-1} increases is dependent on π. For instance, C_S^{-1} values are quite similar for mixed films containing $X_{cer16:0} \leq 0.6$ at low surface pressures (e.g., 5 mN/m) (Fig. 3). In contrast, at high surface pressures in the range thought to mimic biological membranes (i.e., $\pi \geq 30$ mN/m), DMPC can only accommodate

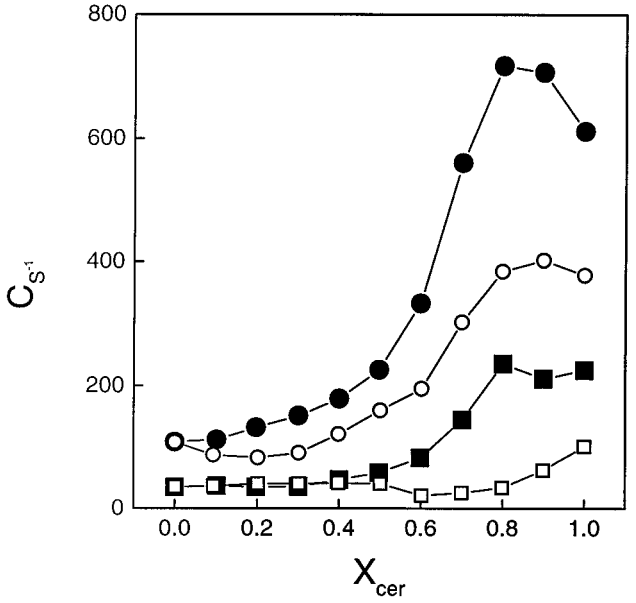

FIGURE 3 C_S^{-1} versus X_{cer} at 5 (■) and 30 mN/m (●). Closed and open symbols denote data for C16:0-ceramide/DMPC and C24:1-ceramide/DMPC mixtures, respectively. The data were taken from the graphs illustrated in Fig. 1, *C* and *D*.

$X_{cer16:0} < 0.4$ before interfacial elasticity begins to decrease (Fig. 3). Further increase in $X_{cer16:0}$ results in an abrupt decrease in interfacial elasticity, so that threefold higher C_S^{-1} values are measured at $X_{cer16:0} = 0.6$, and sevenfold higher at $X_{cer16:0} = 0.8$ (Fig. 3).

We then determined the C_S^{-1} versus A dependency also for DMPC and C24:1-ceramide monolayers (Fig. 1 *D*). The phase transition caused by increasing $X_{cer24:1}$ coincides with a shift of the maximum C_S^{-1} value to larger mean molecular areas at low surface pressures. The minimum value of C_S^{-1} represents the onset of phase separation determined from fluorescence microscopy of DMPC/C24:1-ceramide lipid mixtures (see below). The lack of this minimum/abrupt change (e.g., $X_{cer16:0} = 0.5$ and $X_{cer24:1} = 0.8$) indicates that even at low surface pressures a two-phase coexistence is observed. This allows precise determination of the onset of the phase separation. Similarly to what was observed for DMPC/C16:0-ceramide mixtures at high surface pressures, C_S^{-1} is increased also by C24:1-ceramide. At low surface pressures (e.g., $\pi = 5$ mN/m) no apparent changes are observed in C_S^{-1} upon increasing $X_{cer24:1}$ (Fig. 3). However, at high surface pressures (e.g., $\pi = 30$ mN/m), the maximum C_S^{-1} value decreased slightly for $X_{cer24:1} = 0.2$ (~0.8-fold) compared to the neat DMPC film. Increasing $X_{cer24:1}$ to 0.4 increased C_S^{-1} by 1.1-fold, and further by 1.8-fold at $X_{cer24:1} = 0.6$. The C_S^{-1} values measured for $X_{cer24:1}$ from 0.8 to 1.0 were ~3.5–3.6-fold higher compared to DMPC (Fig. 3).

Fluorescence microscopy of DMPC/ceramide monolayers

In order to aid the interpretation of the force-area isotherms we investigated these films by fluorescence microscopy (Weis, 1994). The fluorescent lipid analog, NBD-PC ($X = 0.01$) readily partitions into the liquid-expanded domains in the coexistence region (Weis and McConnell, 1985). Images of DMPC (Fig. 4, *A–D*) show no indication of lateral phase separation regardless of π, consistent with the liquid-expanded behavior (Fig. 1 *A*). However, at $X_{cer16:0} = 0.5$ lateral phase separation is seen at all surface pressures (Fig. 4, *E–H*). Based on our DSC and x-ray scattering data (Holopainen et al., 2000a) on DMPC/C16:0-ceramide multilamellar vesicles it seems feasible to suggest that the dark domains seen in Fig. 4, *E–H* would represent a solid ceramide enriched phase. Yet, it is also possible that they could be defined as "plastic" domains. To verify the latter possibility requires measurement of the rheological properties of the films. At $X_{cer16:0} = 0.9$ the images show punctate fluorescence, indicative of the dye being excluded from the condensed, single-phase monolayer (Fig. 4, *I--L*). Images of DMPC/C24:1-ceramide (molar ratio 8: 2) monolayer reveal no indications of phase separation at $\pi < 15$ mN/m (Fig. 4, *M* and *N*). However, further increase in π results in the formation of coexisting liquid and condensed phases (*panels O* and *P*). At DMPC/C24:1-ceramide molar ratio of 0.3:0.7 even at low surface pressures (>1–2 mN/m) a two-phase monolayer is evident (Fig. 4, *Q–T*), consistent with the interpretation from compression isotherms (Fig. 1 *B*). Importantly, the domain morphologies for the two ceramides mixed with DMPC are distinctively different. In brief, for mixtures of DMPC with C16:0-ceramide a substantial population of the dark area is connected to form a network-like structure with round dark domains captured within the light areas. In contrast, for DMPC/C24:1-ceramide mixed monolayers the dark domains are arranged into fractal or flower-like patterns. The average number of the petals in the dark flower like domains is quite constant (6.4 ± 0.9).

ΔV versus A behavior of DMPC/ceramide films

To further characterize the effects of ceramide on membrane properties we measured also surface potential-area (ΔV-A) isotherms for both DMPC/C16:0-ceramide and DMPC/C24:1-ceramide films. It should be noted that for these uncharged lipid species ΔV represents the macroscopic average of the membrane dipole potential as a function of A. Taking into account the phase separation evident in fluorescence microscopy images, the interpretation of the ΔV data is thus somewhat limited. Representative ΔV-A isotherms for the DMPC/C16:0-ceramide films are depicted in Fig. 5 *A*. For expanded films of PCs, Phillips and Chapman (1968) found ΔV to increase from ≈270 mV at 1 mN/m to ≈450 mV at 40 mN/m, as measured also for DMPC in this study. To address changes in ΔV more quantitatively due to increasing proportions of C16:0-ceramide, we determined ΔV versus $X_{cer16:0}$ isobars at four different surface pressures, viz. 5, 15, 30, and 40 mN/m (Fig. 5 *B*). Regardless of the value of π a sigmoidal behavior of ΔV versus $X_{cer16:0}$ is evident. At 5 mN/m ΔV is increased from 343 to 531 mV upon increasing $X_{cer16:0}$. However, increasing π diminishes the difference in surface potential observed at $X_{cer16:0} = 0$ and $X_{cer16:0} = 1.0$ (Fig. 5 *B*).

To gain more insight into differences between the two ceramides we also investigated the dependency of ΔV for DMPC/ceramide mixtures on the lipid concentration at constant values of surface pressure. Surface potential ideally varies with concentration, as $\Delta V \propto (\text{area per molecule})^{-1}$. As potentials for different lipids are not simply additive as a function of their concentrations in the membrane (Smaby and Brockman, 1992) the close to ideal behavior (i.e., an almost linear correlation between these two parameters) of C16:0-ceramide/DMPC films in the range $X_{cer16:0} = 0.1$–0.7 (Fig. 6 *A*) thus complies with their immiscibility.

As described by Eq. 1, at any area the potential is independent of the surface pressure. A very different pattern is evident for the binary mixtures of DMPC with C24:1-ceramide (Fig. 5 *C*). To facilitate the viewing of these results we plotted the ΔV versus $X_{cer24:1}$ isobars at four different surface pressures, viz. 5, 15, 30, and 40 mN/m (Fig. 5 *D*). At 5 mN/m increasing $X_{cer24:1}$ up to 0.5 results in a monotonous decrease in ΔV, whereafter a rapid increase in ΔV is observed, reaching ~450 mV for neat C24:1-ceramide. Increasing the surface pressure to 15 mN/m low-

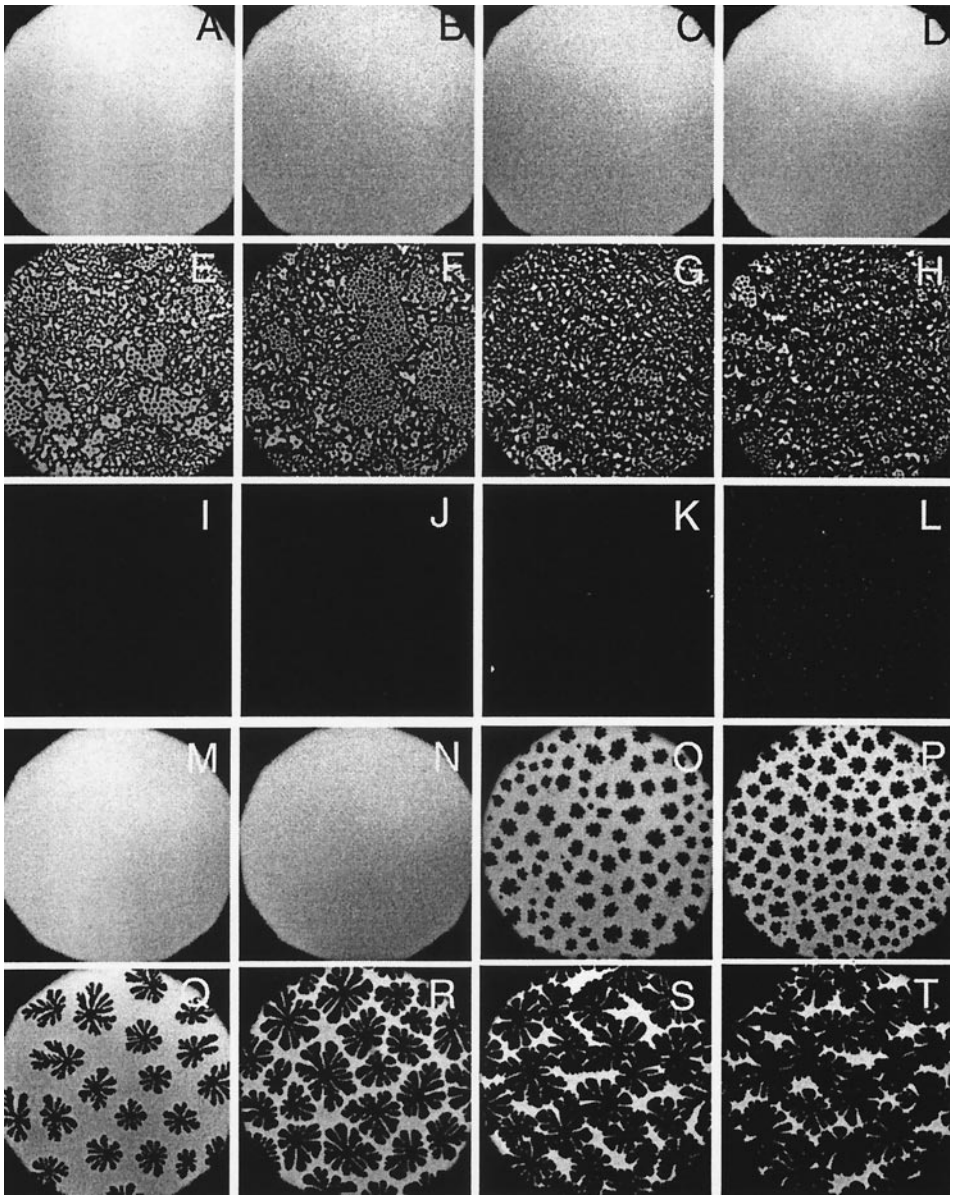

FIGURE 4 Fluorescence microscopy images of a DMPC/NBD-PC (99:1, molar ratio) (*A–D*), DMPC/C16:0-ceramide/NBD-PC (49:50:1, molar ratio) (*E–H*), DMPC/C16:0-ceramide/NBD-PC (9:90:1, molar ratio) (*I–L*), DMPC/C24:1-ceramide/NBD-PC (79:20:1, molar ratio) (*M--P*), and DMPC/C24:1-ceramide/NBD-PC (29:70:1, molar ratio) (*Q–T*), monolayers at surface pressures (from left to right) of 5, 15, 30, and 40 mN/m. Compression rate was 2.5 Å^2/acyl chain/min and the subphase was 10 mM phosphate-saline buffer, 1 M NaCl, pH 6.6. Images were recorded at 24 ± 1°C.

ers the point of discontinuity to $X_{cer24:1} = 0.3$. As surface pressure is increased to 30 mN/m the transition in ΔV is evident already at $X_{cer24:1} = 0.1$. At 40 mN/m the discontinuity can no longer be resolved. Importantly, the emergence of the discontinuities coincides with the emergence of the two-phase region seen by fluorescence microscopy.

The ΔV versus X_{cer} behavior for the two ceramides exhibits a rather different pattern. Although C16:0-ceramide shows a sigmoidal dependency between the two parameters, either a decrease or increase in ΔV is evident for C24:1-ceramide, depending on $X_{cer24:1}$. Likewise, the C24:1-ceramide/DMPC monolayers exhibit clearly different dependency of ΔV on lipid surface concentration (Fig. 6 *B*), in keeping with non-ideal miscibility in the liquid and condensed phases and the presence of the liquid-expanded to condensed phase transition.

DISCUSSION

An informative approach for assessing the lateral interactions of lipids is to determine the molecular area of mixed lipid monolayers as a function of surface pressure. Löfgren and Pascher (1977) showed that ceramides containing a 4,5-*trans* double bond in the long alkyl chain base were condensed into a crystalline assembly, whereas species lacking the double bond were closely packed only at relatively high surface pressures. The area per molecule and compressibility did further depend on the number and configuration of the hydroxyl groups. The N-octadecanoylsphingosine (C18:0-ceramide) revealed expanded to condensed force-area isotherms lacking any additional phase transitions between two mesomorphic states of the lipid monolayer. The small collapse area (39 Å^2) measured for

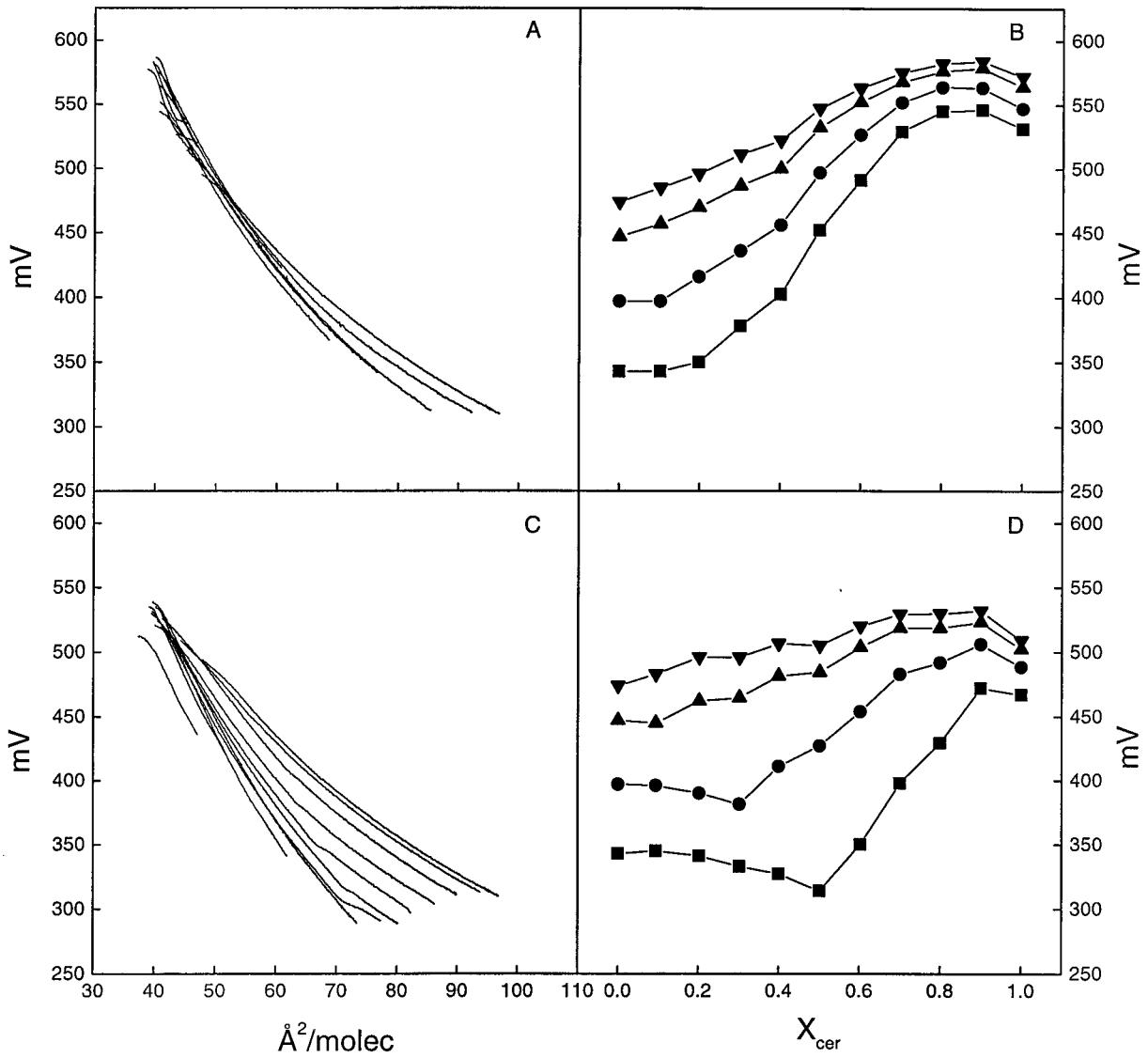

FIGURE 5 (*A*) Representative surface potential ΔV versus mean molecular area plots for pure DMPC and its mixtures with C16:0-ceramide. For the sake of clarity the isotherms are not identified. (*B*) ΔV versus $X_{cer16:0}$ at π: 5 (■), 15 (●), 30 (▲), and 40 (▼) mN/m. Otherwise the conditions were as for Fig. 1 *C*. Surface potential ΔV versus mean molecular area for mixed DMPC and 24:1-ceramide monolayers. (*D*) ΔV versus $X_{cer24:1}$-ceramide at 5 (■), 15 (●), 30 (▲), and 40 mN/m (▼). Otherwise the conditions were similar to Fig. 1. All experiments were repeated at least once to ensure reproducibility. If subsequent isotherms differed >20 mV a third sample was analyzed.

this lipid indicated that the hydrocarbon chains were packed into crystalline arrays with chains perpendicular to the air/water interface thus resembling the monolayer packing of long-chain fatty acids. Interestingly, the surface pressure behavior of C24:1-ceramide closely resembled that of the C18:0-ceramide, the main difference being a lower collapse pressure for the former, suggesting that the longer fatty acid with one *cis* double bond had no effect on the molecular packing (Löfgren and Pascher, 1977). This behavior markedly contrasts those of 18:0 GalCer (galactosylceramide) and 24:1 GalCer, in which the 18:0 GalCer is condensed at all surface pressures below collapse but 24:1 GalCer shows a large two-dimensional phase transition beginning near 10 mN/m (Ali et al., 1993).

The present results were obtained from combined measurements of the cross-sectional area, the interfacial elastic modulus of area compressibility (C_S^{-1}), determination of the changes in surface potential, and fluorescence microscopy, assessing the impact of the N-acyl chain of ceramides on the in-plane interactions in mixed monolayers with DMPC. Although the compression isotherms for monolayers of the neat compounds, C16:0- and C24:1-ceramide were very similar, forming solid condensed films, their mixtures with DMPC were strikingly different. Whereas C16:0-ceramide

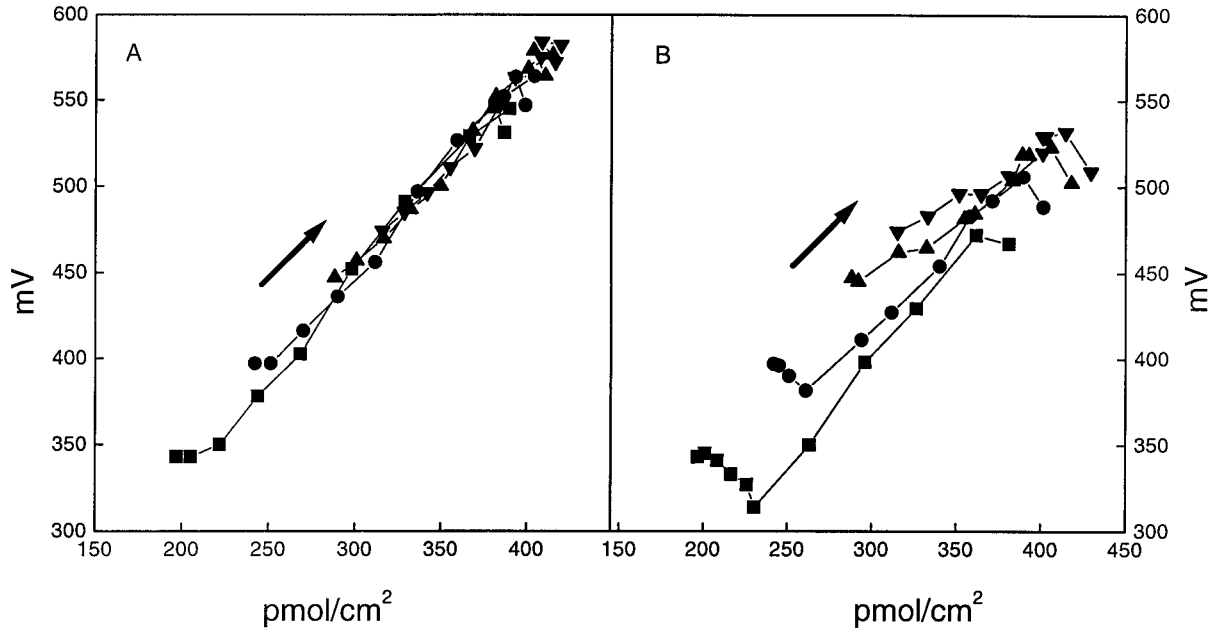

FIGURE 6 Mean molecular area versus lipid concentration for mixed DMPC and C16:0-ceramide (*A*) and DMPC/C24:1-ceramide (*B*) monolayers determined at constant surface pressures of 5 (■), 15 (●), 30 (▲), and 40 mN/m (▼). The data were taken from the graphs illustrated in Figs. 2 (*left*) and 4 *B*, and 2 (*right*) and 4 *D*, respectively. The arrow depicts the direction of increasing $X_{cer16:0}$ or $X_{cer24:1}$.

and DMPC form immiscible pseudo-compounds, C24:1-ceramide and DMPC exhibit surface pressure-dependent miscibility, albeit non-ideal, in both the liquid and condensed phases. Accordingly, the behavior of C16:0-ceramide and C24:1-ceramide in DMPC matrix seem to be governed by different mechanisms. More specifically, whereas for DMPC/C16:0-ceramide interactions (apparent condensation and limited miscibility) are mainly due to the headgroup region of ceramide at all surface pressures, the long N-acyl chain in C24:1-ceramide is likely to diminish the tendency of this lipid for lateral hydrogen bonding (Pascher, 1976; Moore et al., 1997) and thus increase its miscibility with DMPC at low surface pressures. Upon increasing the surface pressure the headgroup interactions dominate and promote lipid immiscibility. The above is most evident in Fig. 6, *A* and *B*, where the correlation of A-ΔV for DMPC/C16:0-ceramide is linear, in contrast to DMPC/C24:1-ceramide.

The in-plane elastic packing interactions have previously been measured by micropipette aspiration technique (e.g., Evans and Needham, 1987). However, this method is applicable only to lipids or lipid mixtures that form large and stable single bilayer vesicles and is thus not feasible for ceramide, for instance. The C_S^{-1} values for chain disordered sphingomyelins (SMs) exceed those for PCs by 25–30% (Smaby et al., 1996), and have been attributed to intermolecular hydrogen bonding of SMs through their amide and hydroxyl groups. In keeping with this the values of C_S^{-1} for ceramides are even higher than for SMs, suggesting further enhanced lateral packing due to hydrogen bonding. C_S^{-1} versus $X_{cer24:1}$ (Fig. 1 *D*) data show a clear discontinuity (dips) at low surface pressures. These discontinuities suggest the formation of phase boundaries at low surface pressure consistent with previous reports (Smaby et al., 1997) and verified here for C24:1-ceramide by fluorescence microscopy showing the appearance of distinct flower-like domains slightly above the dip in C_S^{-1}. The sharp increase in compressibility may reflect the percolation threshold of the two phases. More specifically, when $X_{cer16:0}$ is increased from 0.1 to 0.7 the decrease in compressibility could correspond to the condensed lipid becoming the continuous phase. Accordingly, when the liquid phase is the continuum, lateral compression is transmitted throughout the liquid matrix so that C_S^{-1} increases monotonically with $X_{cer16:0}$. Crossing the percolation threshold the matrix is solid with fluid domains trapped in it. Compression on the solid matrix resists compression of the fluid droplets so the measured compressibility modulus increases dramatically at the percolation threshold. Inspection of the images for $X_{cer16:0} = 0.5$ shows a dark (condensed) continuum at all surface pressures, although at the two lower pressures there are fairly large clusters of dark domains in a fluid matrix. The area compressibility moduli C_S^{-1} for C16:0-ceramide/DMPC mixtures exhibit no minima as a function of decreasing average area, although such minima are known to occur in the two-phase region for pure lipids. Yet, partial immiscibility (or "complex" formation) is indeed suggested by the average area versus composition plots and is evident from the fluorescence microscopy data. Whether this is due to the

small size of the domains or some other property of the pseudo-complex remains unclear at present.

The difference in the mixed films of DMPC with C16:0- and C24:1-ceramide is dramatic and can be attributed solely to their different N-acyl chains. The impact of the C24:1 chain in the DMPC-ceramide film can be rationalized analogously to the "mushroom" → "brush" transition described for grafted polymers (Bijsterbosch et al., 1995; de Gennes, 1980; Hristova and Needham, 1995; Majewski et al., 1998). At low pressures and at low contents of C24:1-ceramide the end of the long C24:1 acyl chain protrudes above the monolayer, adopting a "gaseous" state similar to the "mushroom" conformation of polymers. Accordingly, compared to C16:0-ceramide there is an additional repulsive potential between C24:1-ceramide molecules which promotes its miscibility in DMPC. The average areas in A versus $X_{\mathrm{cer24:1}}$ isobars show film expansion (Fig. 2, *right*). Increasing lateral packing of the film or increasing $X_{\mathrm{cer24:1}}$ causes the protruding "mushrooms" to contact, thus resulting in the protruding part of the C24:1 chain above the monolayer to undergo a transition, viz., decrement in the number of *gauche* bonds, adopting a regime similar to the "brush" conformations for polymers. In this state contacts and hydrogen bonding between C24:1-ceramide molecules are augmented and the mixed film condenses, as seen in the A versus $X_{\mathrm{cer24:1}}$ isobars (Fig. 2, *right*). Compared to C16:0-ceramide for C24:1-ceramide in the "brush" regime there should now be an additional attractive potential due to van der Waals interaction between the protruding acyl chains. The "mushroom" → "brush" transition of the C24:1-ceramide chains is a first-order transition, involving two-phase regions, as verified by fluorescence microscopy. Interactions between the constituent molecules in the DMPC/C24:1-ceramide film are thus different from those composed of DMPC and C16:0-ceramide, resulting in different domain morphologies. The "mushroom" → "brush" transition suggested above should also be readily evident in surface potential values, as indeed it was observed (Figs. 5 and 6). More specifically, as it is the vertical component of the dipole moment that contributes to the measured potentials due to angular averaging, the terminal methyl groups may not contribute to the surface potential when in the "mushroom" conformation. Instead, in the "brush" conformation there should be a significant impact, especially at higher mole fractions of 24:1 ceramide and in the condensed state. Likewise, the compressibility should be high in the "mushroom" regime as well as in the coexistence region, in keeping with our measurements (Fig. 1). Finally, increasing the content of C24:1-ceramide facilitates the formation of microdomains enriched in this lipid.

For C16:0-ceramide the dark ceramide enriched domains exhibit a complex network with some round domains entrapped into the bright continuum. At $X_{\mathrm{cer16:0}} = 0.5$ the amount of circular domains is ~20–30% of the total dark area and the rest is arranged in complex, interconnected networks. The morphology of the C16:0-ceramide is likely to reflect its tight packing and immiscibility in DMPC due to efficient hydrogen bonding. C24:1-ceramide/DMPC films at low ceramide concentrations already exhibit flower-like solid domains that do not fuse, even at high surface pressures. Theoretically, round domains with minimum domain boundaries arise when line tension dominates the energetics of domain morphology. In contrast, domains with complex shapes, such as the flower or networks, are a result of large dipole-dipole repulsion compared to line tension (Perković and McConnell, 1997). The very different domain morphologies evident for the two ceramides mixed with DMPC thus provide strong support for different interactions between the film constituents, as discussed above.

The significance of lipids with long acyl chains is not understood. Our present results demonstrate that the impact of the N-acyl chain in ceramides can be profound. Yet, it still remains to established how the difference evident in the behavior of the monolayers is manifested in bilayers. In the latter the determinants for ordering are more complex, and the possibility of microdomain formation due to hydrophobic mismatch of lipids has to be taken into account as well (Lehtonen et al., 1996). In bilayers, the "brush" regime of C24:1-ceramide would be expected to promote its partial interdigitation with the acyl chains of the adjacent leaflet, causing coupling of the two monolayers. Another ceramide of this type is one with a C26:1 chain, which can be anticipated to behave in a similar manner. In the "mushroom" regime, in contrast, this coupling due to interdigitation would be absent. Similar and perhaps more aggravated behavior in the "brush" regime could be expected for the C24:0- and C26:0-ceramide species. Studies on the further characterization of these lipids are in progress in our laboratory. It has been suggested that C16:0-ceramide represents the ceramide species functioning as the second messenger in apoptosis (Thomas et al., 1999). In light of this study it seems feasible that different ceramide species may serve very different biological functions, determined by their impact on the physical properties on membranes. Although the biological significance of this finding remains unknown, it is possible that the morphology of their domains could have an impact on their differential effects in cellular membranes. Notably, the pronounced differences on the macroscopic scale observed by fluorescence microscopy readily imply equally dramatic differences in the organization of these lipids on shorter length scales as well.

The authors thank J. Smaby, M. Momsen, W. Momsen, and Dr. M. Dahim for many helpful discussions and technical help during this study.

This study was supported by Finnish State Medical Research Council and TEKES (P.K.J.K.), and USPHS Grants HL49180 (H.L.B.) and GM45928 (R.E.B.). J.M.H. is supported by the M.D./Ph.D. program of University of Helsinki.

REFERENCES

Ali, S., J. M. Smaby, and R. E. Brown. 1993. Acyl structure regulates galactosylceramide's interfacial interactions. *Biochemistry.* 32: 11696–11703.

Bijsterbosch, H. D., V. O. de Haan, A. W. de Graaf, M. Mellema, F. A. M. Leermakers, M. A. Cohen Stuart, and A. A. van Well. 1995. Tethered adsorbing chains: neutron reflectivity and surface pressure of spread diblock copolymer monolayers. *Langmuir.* 11:4467–4473.

Brockman, H. L., C. M. Jones, C. J. Schwebke, J. M. Smaby, and D. E. Jarvis. 1980. Application of a microcomputer-controlled film balance system to collection and analysis of data from mixed monolayers. *J. Colloid Interface Sci.* 78:502–512.

Brockman, H. L. 1994. Dipole potential of lipid membranes. *Chem. Phys. Lipids.* 73:57–79.

Carrer, D. C., and B. Maggio. 1999. Phase behavior and molecular interactions in mixtures of ceramide with dipalmitoylphosphatidylcholine. *J. Lipid Res.* 40:1978–1989.

Crisp, D. J. 1949. Two dimensional phase rule. II. Some applications of a two dimensional phase rule for a single surface. *In* Surface Chemistry. Butterworths, London. 23–35.

de Gennes, P. G. 1980. Conformations of polymers attached to an interface. *Macromolecules.* 13:1069–1075.

Elias, P. M., and G. K. Menon. 1991. Structural and lipid biochemical correlates of the epidermal permeability barrier. *Adv. Lipid Res.* 23: 753–758.

Evans, E., and D. Needham. 1987. Physical properties of surfactant bilayer membranes: thermal transitions, elasticity, rigidity, cohesion, and colloidal interactions. *J. Phys. Chem.* 91:4219–4228.

Hannun, Y. A. 1996. Functions of ceramide in coordinating cellular responses to stress. *Science.* 274:1855–1859.

Holopainen, J. M., M. I. Angelova, and P. K. J. Kinnunen. 2000b. Vectorial budding of vesicles by asymmetric enzymatic formation of ceramide in giant liposomes. *Biophys. J.* 78:830–838.

Holopainen, J. M., J. Y. A. Lehtonen, and P. K. J. Kinnunen. 1997. Lipid microdomains in dimyristoylphosphatidylcholine-ceramide liposomes. *Chem. Phys. Lipids.* 88:1–13.

Holopainen, J. M., J. Lemmich, F. Richter, O. G. Mouritsen, G. Rapp, and P. K. J. Kinnunen. 2000a. Dimyristoylphosphatidylcholine/C16:0-ceramide binary liposomes studied by differential scanning calorimetry and wide- and small-angle x-ray scattering. *Biophys. J.* 78:2459–2469.

Holopainen, J. M., M. Subramanian, and P. K. J. Kinnunen. 1998. Sphingomyelinase induced lipid microdomain formation in a fluid phosphatidylcholine/sphingomyelin membrane. *Biochemistry.* 37: 17562–17570.

Hristova, K., and D. Needham. 1995. Phase behavior of a lipid/polymer-lipid mixture in aqueous medium. *Macromolecules.* 28:991–1002.

Kinnunen, P. K. J. 1991. On the principles of functional ordering in biological membranes. *Chem. Phys. Lipids.* 57:375–399.

Kinnunen, P. K. J., A. Koiv, J. Y. A. Lehtonen, M. Rytömaa, and P. Mustonen. 1994. Lipid dynamics and peripheral interactions of proteins with membrane surfaces. *Chem. Phys. Lipids.* 73:181–207.

Kinnunen, P. K. J., and P. Laggner (Eds.). 1991. Phospholipid phase transitions. Special issue in *Chem. Phys. Lipids.* 57:109–408.

Kolesnick, R. N. 1991. Sphingomyelin and derivatives as cellular signals. *Prog. Lipid Res.* 30:1–38.

Lehtonen, J. Y. A., J. M. Holopainen, and P. K. J. Kinnunen. 1996. Evidence for the formation of microdomains in liquid crystalline large unilamellar vesicles caused by hydrophobic mismatch of the constituent phospholipids. *Biophys. J.* 70:1753–1760.

Lisanti, M. P., P. E. Scherer, Z. Tang, and M. Sargiacomo. 1994. Caveolae, caveolin and caveolin-rich membrane domains: a signalling hypothesis. *Trends Cell Biol.* 4:231–235.

Liu, P., and R. G. Anderson. 1995. Compartmentalized production of ceramide at the cell surface. *J. Biol. Chem.* 270:27179–27185.

Löfgren, H., and I. Pascher. 1977. Molecular arrangements of sphingolipids. The monolayer behaviour of ceramides. *Chem. Phys. Lipids.* 20: 273–284.

Majewski, J., T. L. Kuhl, K. Kjaer, M. C. Gerstenberg, J. Als-Nielsen, J. N. Israelachvili, and G. S. Smith. 1998. X-ray synchrotron study of packing and protrusion of polymer-lipid monolayers at the air-water interface. *J. Am. Chem. Soc.* 120:1469–1473.

Majno, G., and I. Joris. 1995. Apoptosis, oncosis, and necrosis. An overview of cell death. *Am. J. Pathol.* 146:3–19.

Moore, D. J., M. E. Rerek, and R. Mendelsohn. 1997. FTIR spectroscopy studies of the conformational order and phase behaviour of ceramides. *J. Phys. Chem. B.* 101:8933–8940.

Mouritsen, O. G., and P. K. J. Kinnunen. 1996. Role of lipid organization and dynamics for membrane functionality. *In* Biological Membranes. K. Merz, Jr., and B. Roux, editors. Birkhäuser, Boston. 463–502.

Parton, R. G., B. Joggerst, and K. Simons. 1994. Regulated internalization of caveolae. *J. Cell Biol.* 127:1199–1215.

Pascher, I. 1976. Molecular arrangements in sphingolipids. Conformation and hydrogen bonding of ceramide and their implication on membrane stability and permeability. *Biochim. Biophys. Acta.* 455:433–451.

Perković, S., and H. M. McConnell. 1997. Cloverleaf monolayer domains. *J. Phys. Chem. B.* 101:381–388.

Phillips, M. C., and D. Chapman. 1968. Monolayer characteristics of saturated 1,2-diacyl phosphatidylcholines (lecithins) and phosphatidylethanolamines at the air-water interface. *Biochim. Biophys. Acta.* 163:301–313.

Radhakrishnan, A., and H. M. McConnell. 1999. Cholesterol-phospholipid complexes in membranes. *J. Am. Chem. Soc.* 121:486–487.

Shah, J., J. M. Atienza, R. I. Duclos, Jr., A. V. Rawlings, Z. Dong, and G. G. Shipley. 1995. Structural and thermotropic properties of synthetic C16:0 (palmitoyl) ceramide: effect of hydration. *J. Lipid Res.* 36: 1936–1944.

Smaby, J. M., and H. L. Brockman. 1990. Surface dipole moments of lipids at the argon-water interface. Similarities among glycerol-ester-based lipids. *Biophys. J.* 58:195–204.

Smaby, J. M., and H. L. Brockman. 1992. Characterization of lipid miscibility in liquid-expended monolayers at the gas-liquid interface. *Langmuir.* 8:563–570.

Smaby, J. M., V. S. Kulkarni, M. Momsen, and R. E. Brown. 1996. The interfacial elastic packing interactions of galactosylceramides, sphingomyelins, and phosphatidylcholines. *Biophys. J.* 70:868–877.

Smaby, J. M., M. Momsen, V. S. Kulkarni, and R. E. Brown. 1997. Phosphatidylcholine acyl unsaturation modulates the decrease in interfacial elasticity induced by cholesterol. *Biophys. J.* 73:1492–1505.

Thomas, R. L., Jr., C. M. Matsko, M. T. Lotze, and A. A. Amoscato. 1999. Mass spectrometric identification of increased C16 ceramide levels during apoptosis. *J. Biol. Chem.* 274:30580–30588.

Veiga, M. P., J. L. R. Arrondo, F. M. Goñi, and A. Alonso. 1998. Ceramides in phospholipid membranes: effects on bilayer stability and transition to nonlamellar phases. *Biophys. J.* 76:342–350.

Weis, R. M. 1994. Fluorescence microscopy of phospholipid monolayer phase transitions. *Chem. Phys. Lipids.* 57:227–239.

Weis, R. M., and H. M. McConnell. 1985. Cholesterol stabilizes the crystal-liquid interface in phospholipid monolayers. *J. Phys. Chem.* 89:4453–4459.